Contactless Antenna Radiation Efficiency Measurement Within Reverberation Chambers: Sensitivity Improvement

Francois Sarrazin, Adnane Labdouni, Wafa Krouka, Julien de Rosny, Elodie Richalot

Contactless Antenna Radiation Efficiency Measurement Within Reverberation Chambers: Sensitivity Improvement

François Sarrazin[#1], Adnane Labdouni[#2], Wafa Krouka[#3], Julien de Rosny[*4], Elodie Richalot[#5]

[#]Univ Gustave Eiffel, CNRS, ESYCOM, F-77454 Marne-la-Vallée, France

[*]ESPCI Paris, PSL Research University, CNRS, Institut Langevin, F-75005 Paris, France

{[1]francois.sarrazin, [2]adnane.labdouni, [3]wafa.krouka, [5]elodie.richalot-taisne}@univ-eiffel.fr, [4]julien.derosny@espci.psl.eu

***Abstract* — This paper discusses the sensitivity improvement of a contactless antenna radiation efficiency measurement method within reverberation chambers (RCs). The method does not need to connect the antenna under test to an analyzer through cables, which are known to disturb antenna impedance and radiation characteristics when placed in the reactive field zone of electrically small antennas. The sensitivity improvement is achieved through the use of multiple identical AUTs located within the RC in order to enhance the quality factor variation introduced by the modification of the AUT load impedance.**

***Keywords* — antenna, antenna measurement, backscattering measurement, contactless, reverberation chamber, radiation efficiency.**

I. Introduction

As part of the Internet of Things and other 5G-and-beyond applications, electrically small antennas (ESAs) are of great interest in order to be integrated into small wireless devices, such as communicating sensors. In addition to antenna size reduction and efficiency optimization [1], bounded by physical limits, ESAs characterization is also a major challenge. Indeed, during conventional transmission-type measurement, the presence of measurement cables in the reactive field zone of an antenna disturbs both its impedance and radiation characteristics [2], especially when dealing with ESAs. Moreover, due to ESA limited ground plane size, the cable itself acts as a radiator, artificially increasing the antenna radiation efficiency [3]. Two ways have been investigated to overcome this issue: 1) reducing the cable effect by adding ferrites [4] or baluns [5], and 2) avoiding the use of measurement cables by performing backscattering measurement.

Non-invasive methods, i.e., which avoid the use of measurement cables, have been proposed in the literature but only in order to retrieve antenna radiation pattern. They are based on backscattering measurement for at least two antenna load impedances (load modulation) and have been performed first in anechoic chamber [6] and very recently in reverberation chambers (RCs) [7]. However, antenna radiation efficiency, which is one of ESA most critical parameter, can hardly be assessed by such techniques. Indeed, they require to measure the entire antenna radiation pattern (over a sphere), making these techniques highly time-consuming.

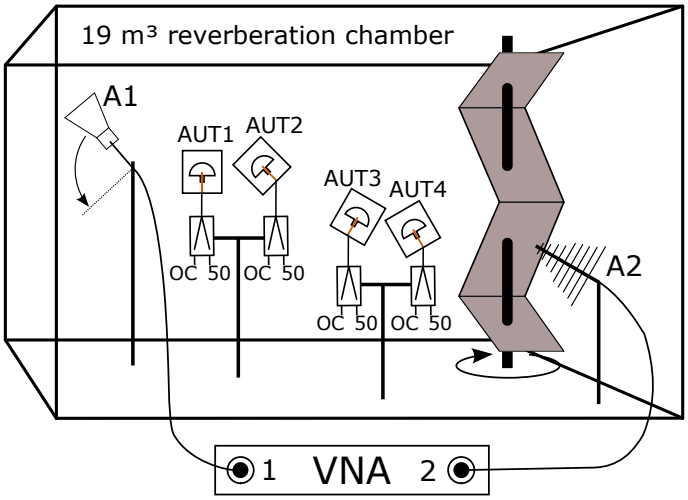

Fig. 1. Measurement setup within the 19 m^3 RC of ESYCOM. A1 and A2 are a horn antenna and a log-periodic antenna, respectively, connected to a VNA. The AUT is a printed wideband slot antenna. Each one of the 4 identical AUTs is connected to a remotely-controlled switch enabling to choose between an open circuit and a 50 Ω load.

In 2021, a contactless antenna radiation efficiency measurement method has been proposed [8] combining advantages of both scattering measurement, i.e., a non-invasive measurement setup, and conventional RC measurement techniques, i.e., neither antenna under test (AUT) alignment issues nor rotation [9], [10]. The method is based on RC Q-factor measurement for two different AUT load conditions. Then, using a recent model of antenna Q-factor introduced in [11], the AUT radiation efficiency can be retrieved.

The sensitivity of this method relies on the RC Q-factor variation due to the modification of the AUT loading condition. However, this variation may appear to be low in the case of poorly efficient antenna and/or at high frequencies. In this paper, we propose a technique to increase the sensitivity of the contactless antenna radiation efficiency measurement method. It is based on the use of several identical AUTs, which will enhance the measured RC Q-factor variation. Section II briefly recalls the contactless measurement method whereas Section III presents measurement results and analyses.

II. Measurement Method

The RC Q-factor $Q_{\mathrm{L}x}$, in the presence of N AUTs terminated by the same load impedance Lx, can be expressed as:

$$Q_{\mathrm{L}x}^{-1} = Q_{\mathrm{c}}^{-1} + NQ_{\mathrm{a,L}x}^{-1} \tag{1}$$

where $Q_{\mathrm{a,L}x}$ is the AUT Q-factor (terminated by the load impedance Lx) and Q_{c} is the Q-factor of the chamber including all losses but the AUT ones (wall, stirrer, measurement antennas...). If we consider two measurements for two AUT load impedances, namely L1 and L2, it comes:

$$Q_{\mathrm{L1}}^{-1} - Q_{\mathrm{L2}}^{-1} = N\left(Q_{\mathrm{a,L1}}^{-1} - Q_{\mathrm{a,L2}}^{-1}\right) \tag{2}$$

The term Q_{c}^{-1} being identical for both measurements, it vanishes in (2). A definition of the antenna Q-factor $Q_{\mathrm{a,L}x}^{-1}$ has been first proposed by Hill [12] before being refined in [11] by taking into account the power reflected back by the antenna towards the chamber:

$$Q_{\mathrm{a,L}x} = \frac{Q_{\mathrm{a}}^{0}}{1 - \eta_{\mathrm{rad}}^{2}\left|\Gamma_{\mathrm{a,L}x}\right|^{2}}. \tag{3}$$

where $\Gamma_{\mathrm{a,Lx}}$ with $x = \{1, 2\}$ is the reflection coefficient between the AUT and its load impedance Lx, and $Q_{\mathrm{a}}^{0} = 16\pi^{2}V/\lambda^{3}$ is the Q-factor of an ideal perfectly-matched lossless antenna. Then, by substituting $Q_{\mathrm{a,L}x}$ in (2) by its expression from (3), the AUT radiation efficiency η_{rad} can be expressed as:

$$\eta_{\mathrm{rad}} = \sqrt{\frac{Q_{\mathrm{a}}^{0}\left(Q_{\mathrm{L1}}^{-1} - Q_{\mathrm{L2}}^{-1}\right)}{N\left(\left|\Gamma_{\mathrm{a,L2}}\right|^{2} - \left|\Gamma_{\mathrm{a,L1}}\right|^{2}\right)}}. \tag{4}$$

III. Results

A. Measurement setup

The proposed measurement setup is presented in Fig. 1 and implies the use of a 19 m^3 RC, equipped with a z-fold rotating mechanical mode stirrer. Two measurement antennas (A1 and A2) are connected to a VNA in order to measure the transmission coefficient S_{21} in the 1.8 GHz to 2.8 GHz frequency range (10001 frequency points, IF 10 kHz). A1 is double-ridged broadband horn antenna (Schwarzbeck BBHA 9120 B) and A2 is a log-periodic antenna (Schwarzbeck VUSLP 9111). A1 is oriented towards an edge of the RC whereas A2 is oriented towards the mechanical mode stirrer. They are facing opposite directions in order to avoid direct coupling between them. The AUT is a printed wide-band antenna based on a circular slot excited by a monopole as presented in Fig. 2. This antenna is well matched in the considered 1.8 GHz to 2.8 GHz frequency range. It is connected, through a 50-cm-long coaxial cable, to a remotely-controlled mechanical switch, allowing to choose between an open circuit (OC) and a 50 Ω load. Two experiments are performed: 1) $N = 1$ AUT is placed within the RC working volume, and 2) $N = 4$ AUTs are placed within the RC working volume (as can be seen in Fig. 1). It is noted that all 4 switches and cables are present inside the RC during both experiments, i.e., even in the case of $N = 1$ AUT, in order to keep the Q-factor as similar as possible.

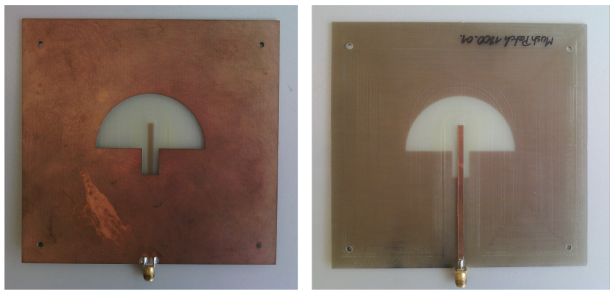

Fig. 2. Picture of the wideband slot-based antenna under test: top view (left) and bottom view (right).

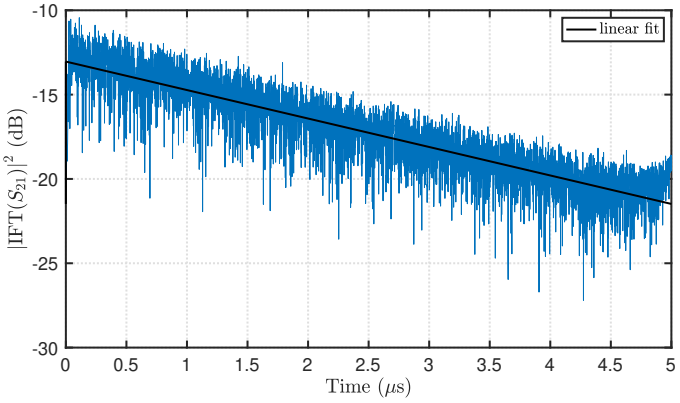

Fig. 3. Power delay profile in dB as a function of time. The RC decay time constant τ_{RC} can be deduced from its slope thanks to a linear fit between 0.5 μs and 3.5 μs.

Three stirring techniques are applied in order to increase the uncorrelated sample size: 1) Mechanical stirring: 72 equally-spaced positions of the mechanical stirrer have been considered; 2) Source stirring: 17 different orientations of A1 have been considered, all of them facing a corner of the RC, and therefore avoiding direct coupling with A2; 3) AUT stirring (also referred as platform stirring): 3 different configurations have been considered, both AUT orientations and positions being changed for each configuration.

B. Q-factor

The RC Q-factor is estimated in the time domain thanks to the relation $Q = \omega\tau_{RC}$. The RC time decay constant τ_{RC} can be retrieved by performing a linear fitting of the power delay profile (PDP) [13] defined as $\mathrm{PDP} = \left\langle \left|\mathrm{IFT}\left(S_{21}\right)\right|^{2} \right\rangle$, where $\langle\cdot\rangle$ refers to the ensemble average over the stirring process, and IFT stands for inverse Fourier transform. Indeed, the PDP decreases with a $1/\tau_{RC}$ slope (Fig. 3).

RC Q-factors for both AUT load conditions (OC and 50 Ω) of each of both experiments ($N = 1$ and $N = 4$) are computed. It is noted that in the case of $N = 4$ AUTs, all AUTs are connected to the same load (either an OC or a 50 Ω load). Q-factors for $N = 4$ AUTs are presented in Fig. 4 (left

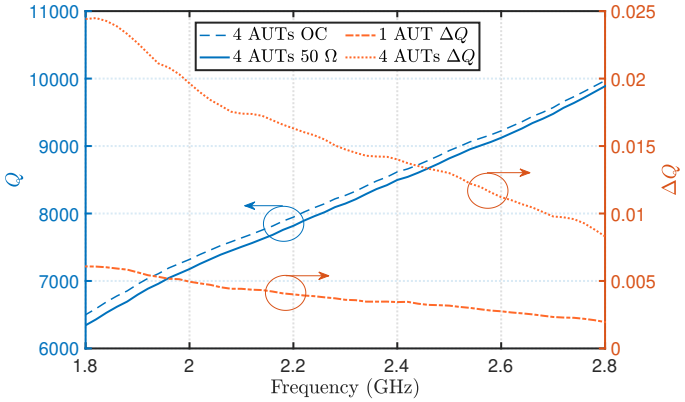

Fig. 4. Q and ΔQ as a function of frequency for the two measurements and two load conditions.

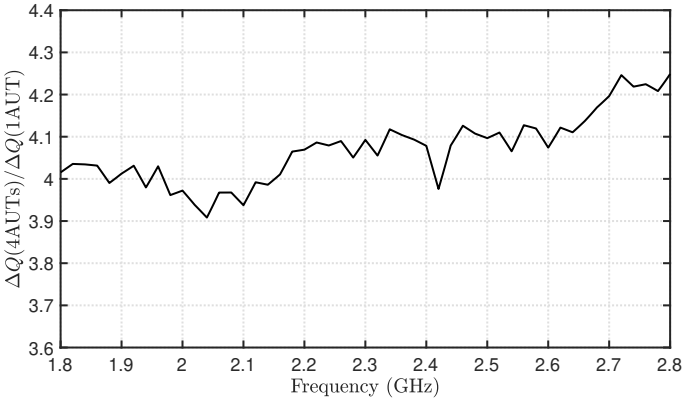

Fig. 5. Ratio of ΔQ for $N = 4$ AUTs and $N = 1$ AUT as a function of frequency.

y-axis). It is observed that the Q-factor for the 50 Ω case is lower than for the OC case as more energy is absorbed by the 50 Ω load. Indeed, the AUT is well matched to 50 Ω in this frequency range. To better evaluate the Q-factor variation due to the AUT load impedance modification, we computed the relative difference ΔQ between OC and 50 Ω, so that $\Delta Q = 2(Q_{50}^{-1} - Q_{OC}^{-1})/(Q_{50}^{-1} + Q_{OC}^{-1})$. Results are presented on the right axis of Fig. 4 for the two experiments ($N = 1$ AUT and $N = 4$ AUTs). We can see that ΔQ decreases as a function of frequency as the contribution of antenna losses in the overall Q-factor decreases. Also, ΔQ is much higher in the case of 4 AUTs than for 1 AUT.

In order to evaluate the impact of the number of AUTs on the Q-factor, the ratio between the two ΔQ is presented in Fig. 5 as a function of frequency. We can see that it ranges from 3.91 to 4.24 and is equal to 4.068 on average. This is consistent with the number of AUTs ($N = 4$). Therefore, it is confirmed here that it is possible to increase the RC Q-factor variation due to the AUT load modification, and therefore the measurement sensitivity, by using multiple identical AUTs. This is especially interesting for the characterization of low-efficiency antennas such as ESAs, for which the RC Q-factor variation may be small, and therefore difficult to assess, according to (3).

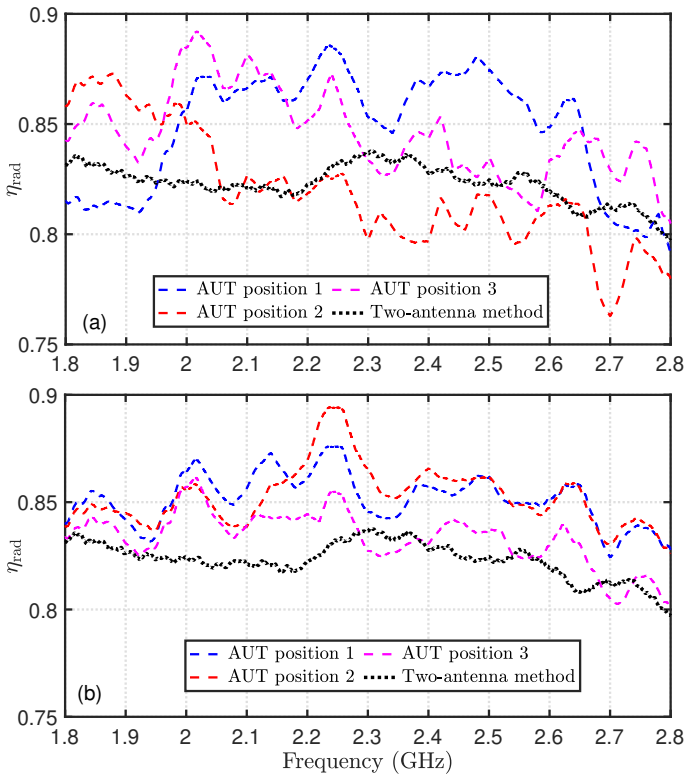

Fig. 6. Radiation efficiency as a function of frequency estimated with the contactless method and compared with the one obtained using the reference two-antenna method, (a) Case with 1 AUT, and (b) Case with 4 AUTs.

C. Radiation Efficiency

Once the RC Q-factors for the two load impedances are known, radiation efficiencies can be estimated thanks to (4). They are presented in Fig. 6(a) in the case of $N = 1$ AUT and in Fig. 6(b) in the case of $N = 4$ AUTs as a function of frequency. Radiation efficiency is evaluated for each AUT position separately which leads to three different estimations, each of them taking advantage from both mechanical and source stirring. They are compared to the estimation using the widely-used *two-antenna method* [13], implemented within the same RC, and is considered here as a reference.

First, we can notice that all contactless estimations are consistent with the reference measurement with a maximum absolute difference of 6.5%, and can be considered within the measurement uncertainty budget [13]. In order to deeper analyze the discrepancies between all radiation efficiency estimations, we compute the normalized standard deviation $\sigma_{\eta_{\rm rad}} / \langle \eta_{\rm rad} \rangle$; results averaged over the frequency bandwidth are presented in Tab. 1. It is equal to 0.0308 in the case of $N = 1$ AUT and equal to 0.0127 in the case of $N = 4$ AUTs. Therefore, the normalized standard deviation is divided by a factor close to 2 when increasing the number of AUT from 1 to 4. According to [14], the normalized standard deviation can be related to the effective number of uncorrelated RC configurations $N_{\rm eff}$ as:

Table 1. Normalized standard deviation of the radiation efficiency estimations averaged over the frequency bandwidth.

$N = 1$ AUT	$N = 4$ AUTs
0.0308	0.0127

$$\frac{\sigma_{\eta_\mathrm{a}}}{\langle \eta_\mathrm{a} \rangle} \approx \sqrt{\frac{2}{N_\mathrm{eff}}}. \tag{5}$$

If we neglect the coupling between the 4 AUTs, we can consider that having 4 AUTs instead of one is equivalent to multiplying N_eff by 4. This leads to a normalized standard deviation theoretically divided by two, which is coherent with our results. This validates the potential interest of increasing the number of identical AUTs in order to lower the measurement uncertainties of the contactless measurement method.

IV. Conclusion

A contactless radiation efficiency measurement method within RCs has been introduced recently in [8] which enables to assess the radiation efficiency of an antenna without connecting it to any analyzer. Therefore, it avoids the use of long cables known to disturb the antenna impedance and radiation characteristics, especially in the case of electrically small antennas. The method is based on the retrieval of the RC Q-factor variation induced by the modification of the AUT load impedance. Such variation being potentially small, this paper introduced a technique to enhance the sensitivity of the contactless method by using multiple identical AUTs in order to increase the RC Q-factor variation, and thus permit its accurate detection even in the case of low-efficiency antennas. The use of 4 AUTs leads to a normalized standard deviation of the estimated radiation efficiency divided by 2 compared to the use of only 1 AUT. It is noted that the normalized standard deviation has been computed thanks to the only three different realizations that have been performed using our specific measurement setup.

Future works will include the evaluation of the measurement uncertainties of the contactless method compared to conventional transmission-type ones, as well as the measurement of low-efficiency antennas in order to point out potential sensitivity limits.

References

[1] F. Sarrazin, S. Pflaum, and C. Delaveaud, "Radiation efficiency improvement of a balanced miniature ifa-inspired circular antenna," *IEEE Antennas and Wireless Propagation Letters*, vol. 16, pp. 1309–1312, 2017.

[2] J. DeMarinis, "The antenna cable as a source of error in emi measurements," in *IEEE 1988 International Symposium on Electromagnetic Compatibility*, 1988, pp. 9–14.

[3] L. Huitema, C. Delaveaud, and R. D'Errico, "Impedance and radiation measurement methodology for ultra miniature antennas," *IEEE Transactions on Antennas and Propagation*, vol. 62, no. 7, pp. 3463–3473, 2014.

[4] C. Icheln, J. Ollikainen, and P. Vainikainen, "Reducing the influence of feed cables on small antenna measurements," *Electronics Letters*, vol. 35, pp. 1212–1214, 1999.

[5] T. Fukasawa, N. Yoneda, and H. Miyashita, "Investigation on current reduction effects of baluns for measurement of a small antenna," *IEEE Transactions on Antennas and Propagation*, vol. 67, no. 7, pp. 4323–4329, 2019.

[6] W. Wiesbeck and E. Heidrich, "Wide-band multiport antenna characterization by polarimetric RCS measurements," *IEEE Transactions on Antennas and Propagation*, vol. 46, no. 3, pp. 341–350, 1998.

[7] A. Reis, F. Sarrazin, P. Besnier, P. Pouliguen, and E. Richalot, "Contactless antenna gain pattern estimation from backscattering coefficient measurement performed within reverberation chambers," *IEEE Transactions on Antennas and Propagation*, pp. 1–1, 2021.

[8] W. Krouka, F. Sarrazin, J. d. Rosny, A. Labdouni, and E. Richalot, "Antenna radiation efficiency estimation from backscattering measurement performed within reverberation chambers," *IEEE Transactions on Electromagnetic Compatibility*, pp. 1–8, 2021.

[9] W. Krouka, F. Sarrazin, J. Sol, P. Besnier, and E. Richalot, "Comparison of antenna radiation efficiency measurement techniques in reverberation chamber using or not a reference antenna," in *2020 14th European Conference on Antennas and Propagation (EuCAP)*, 2020, pp. 1–4.

[10] ——, "Biased estimation of antenna radiation efficiency within reverberation chambers due to unstirred field: Role of antenna stirring," *IEEE Transactions on Antennas and Propagation*, pp. 1–1, 2022.

[11] A. Cozza, "Power loss in reverberation chambers by antennas and receivers," *IEEE Transactions on Electromagnetic Compatibility*, vol. 60, no. 6, pp. 2041–2044, 2018.

[12] D. Hill, "Electromagnetic theory of reverberation chambers," 1998. [Online]. Available: https://tsapps.nist.gov/publication/get_pdf.cfm?pub_id=24427

[13] C. L. Holloway, H. A. Shah, R. J. Pirkl, W. F. Young, D. A. Hill, and J. Ladbury, "Reverberation chamber techniques for determining the radiation and total efficiency of antennas," *IEEE Transactions on Antennas and Propagation*, vol. 60, no. 4, pp. 1758–1770, 2012.

[14] X. Chen, "On statistics of the measured antenna efficiency in a reverberation chamber," *IEEE Transactions on Antennas and Propagation*, vol. 61, no. 11, pp. 5417–5424, 2013.